
Self-Sustained Spin-Polarized Current Oscillations in Multiquantum Well Structures

M. Carretero^{1,2}, L.L. Bonilla^{1,2}, R. Escobedo³ and G. Platero⁴

¹ G. Millán Institute, Fluid Dynamics, Nanoscience & Industrial Mathematics, Universidad Carlos III, 28911 Leganés, Spain, manuel.carretero@uc3m.es

² Unidad Asociada al Instituto de Ciencia de Materiales de Madrid, CSIC, 28049 Cantoblanco, Spain, bonilla@ing.uc3m.es

³ Departamento de Matemática Aplicada y Ciencias de la Computación, Universidad de Cantabria, 39005 Santander, Spain, escobedo@unican.es

⁴ Instituto de Ciencia de Materiales de Madrid, CSIC, 28049 Cantoblanco, Spain
gplatero@csic.es

Summary. A semiconductor multiquantum well structure exhibits self-sustained spin-polarized current oscillations if one or more of its wells are doped with Mn. Analysis and numerical solution of a nonlinear spin transport model yield the minimal number of wells and the range of doping density needed to find oscillations.

1 Introduction

Spintronics is a multidisciplinary field whose central theme is the active manipulation of spin degrees of freedom in solid states systems. Among the fields that are involved in spintronics, magnetoelectronics has achieved important results regarding magnetoresistive effects which are important since they can be used for magnetic read heads in computer hard drives and non-volatile random access memory [1]. Semiconducting materials offer the possibility of new device functionalities not realizable in metallic systems. In particular, Diluted Magnetic Semiconductors (DMS) with nonlinear current-voltage characteristics can be associated with non-magnetic semiconductors to produce efficient spin injectors [2, 3] or be used as spin oscillators [4, 5]. The present work models a dc voltage biased II-VI semiconductor Multiquantum Well Structure (MQWS) attached to normal contacts with at least one quantum well (QW) doped with Mn, thereby constituting a DMS. An external magnetic field causes splitting of energy levels in the DMS and this induces spin polarization in the MQWS. We find that MQWS with at least four QWs exhibit Self Sustained Current Oscillations (SSCOs) that can be used to design spin oscillators. There are interesting spatio-temporal patterns for long MQWS.

2 Governing Equations

2.1 Theoretical Model

The sample under consideration consists of an n-doped ZnSe/(Zn,Cd,Mn)Se weakly coupled MQWS. Under an external magnetic field B , the DMS in QWs doped with Mn^{++} (with spin $S = 5/2$) have spin-dependent energy levels: $E_j^\pm = E_j \mp \Delta/2$ for electron spin $s = \pm 1/2$. The level splitting Δ is a function of B and the Mn density [3], and we can consider it as a tunable parameter.

The governing equations describing our model [5], for a MQWS of N wells, are:

$$F_i - F_{i-1} = \frac{e}{\varepsilon} (n_i^+ + n_i^- - N_D), \quad (1)$$

$$e \frac{dn_i^\pm}{dt} = J_{i-1 \rightarrow i}^\pm - J_{i \rightarrow i+1}^\pm \pm \frac{n_i^- - n_i^+ / \Theta_i}{\tau_{sf}}, \quad (2)$$

$$\Theta_i = 1 + e^{\frac{E_{1,i}^- - \mu_i^+}{\gamma_\mu}}, \quad (3)$$

where $i = 1, \dots, N$. Here n_i^+ , n_i^- and $-F_i$ are the two-dimensional (2D) spin-up and spin-down electron densities, and the average electric field at the i th MQWS period, respectively. The voltage bias condition is $\sum_{i=0}^N F_i l = V$ for an applied voltage V . We have denoted the spin-dependent subband energies (E) by $E_{j,i}^\pm = E_j \mp \Delta_i/2$, with $\Delta_i = \Delta$ or 0, depending on whether the i th well contains magnetic impurities. N_D , ε , $-e$, l , τ_{sf} and $-J_{i \rightarrow i+1}^\pm$ are the 2D doping density at the QWs, the average permittivity, the electron charge, the width of a MQWS period, the spin-flip scattering time, and the tunneling current density across the i th barrier, respectively. For numerical convenience, the right hand side of (2) contains a smoothed form of the scattering term used in [3]. Time-differencing (1) and inserting (2) in the result, we obtain the following form of Ampère's law,

$$\varepsilon \frac{dF_i}{dt} + J_{i \rightarrow i+1} = J(t) = \frac{1}{N+1} \sum_{i=0}^N J_{i \rightarrow i+1}, \quad (4)$$

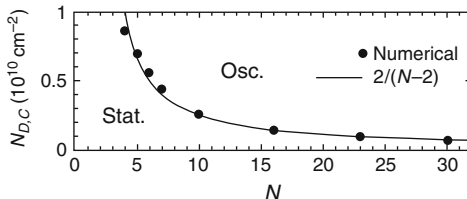


Fig. 1. Minimal doping density N_D for SSCO vs the number of wells N for $\Delta = 15$ MeV

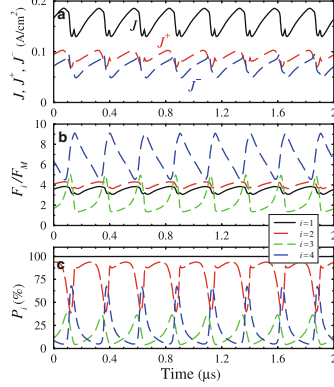


Fig. 2. (a) Tunneling current, (b) electric field and (c) polarization, as a function of time at the i QW during SSCOs for $N = 4$. Solid line ($i = 1$); dot-dashed ($i = 2$); dashed ($i = 3$); long-dashed ($i = 4$)

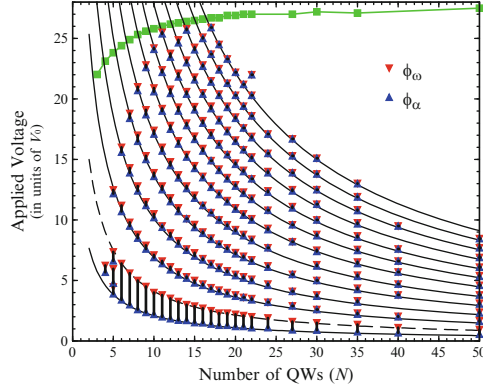


Fig. 3. Phase diagram of average electric field ϕ vs N for a MQWS containing Mn in its first QW. The SSCOs begin at triangles ϕ_α and end at inverted triangles ϕ_ω

where $J_{i \rightarrow i+1} = J_{i \rightarrow i+1}^+ + J_{i \rightarrow i+1}^-$. In (4), $J(t)$ is the total current density. Tunneling currents are calculated taking into account that spin up and down electrons have different energies:

$$J_{i \rightarrow i+1}^\pm = \frac{e v^{(f)\pm}(F_i)}{l} \left\{ n_i^\pm - a \ln \left[1 + e^{-\frac{e F_i l}{k_B T}} \left(e^{\frac{n_{i+1}^\pm}{a}} - 1 \right) \right] \right\}, \quad (5)$$

for $i = 1, \dots, N-1$, with $a = \frac{m^* k_B T}{2\pi\hbar^2}$ [6]. As boundary tunnelling currents for $i = 0$ and N , we use (5) with $n_0^\pm = n_{N+1}^\pm = \kappa N_D/2$ [3]. Initially, we set $F_i = V/[l(N+1)]$, $n_i^\pm = N_D/2$, $v^{(f)\pm}(F_i)$ is the “forward tunneling velocity”, see details in [6]. The currents $J_{i \rightarrow i+1}^\pm$ are functions of F_i , n_i^\pm and n_{i+1}^\pm . For constant values $n_i^\pm = N_D/2$ and $F_i = F$, the tunneling current density at a nonmagnetic QW has a maximum J_M at a value F_M of the field. In terms of

F_M , the voltage bias condition can be written as a condition for the average field ϕ :

$$\frac{1}{(N+1)F_M} \sum_{i=0}^N F_i = \phi \equiv \frac{V}{V_0} = \frac{V}{(N+1)F_M l}. \quad (6)$$

3 Results

3.1 Short Devices: Spin Injector

Nonmagnetic MQWSs do not exhibit SSCOs: at least one QW has to contain magnetic impurities (Mn). Let that QW be the first one, next to the injecting contact. Figure 1 shows that the MQWS should have at least four QWs and sufficient doping density ($N > N_{DC}$) for SSCOs to exist. The critical doping density is approximately given by $N_{DC} = \frac{2}{N-2} \times 10^{10} \text{ cm}^{-2}$.

Figure 2 shows the time evolution of the spin-polarized current densities, the electric field and the spin polarization (defined as $P_i = (n_i^+ - n_i^-)/(n_i^+ + n_i^-)$) at the different periods of a 4-well MQWS with normal contacts. SSCOs are caused by repeated nucleation and motion of electric field pulses which are charge dipole waves. During one oscillation period, the first QW is fully polarized, the second QW is highly polarized and the third and the fourth QWs are strongly polarized when the dipole wave is traversing them. These results should be useful to build an oscillatory spin polarized current injector.

3.2 Long Devices: Spatio-Temporal Patterns

For typical values of the parameters (see [5]) our model exhibits a variety of stationary states with electric file domains (EFD) and SSCOs.

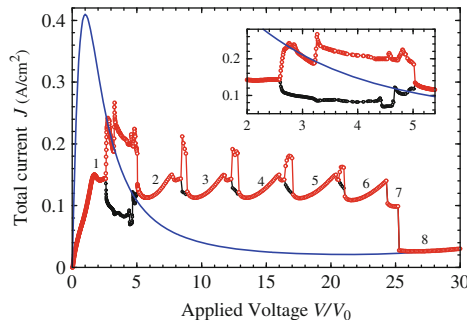


Fig. 4. Current-voltage characteristics for a 8-period MQWS. The maximum and minimum of the SSCOs has been represented with *circles* in each voltage interval where they exist

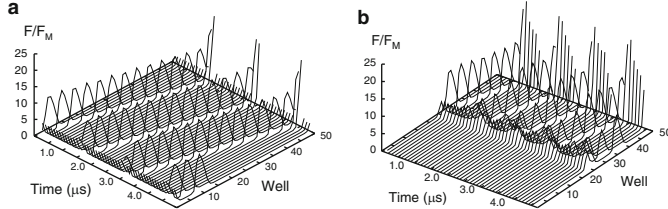


Fig. 5. Electric field profile vs QW index and time for $N = 50$, during SSCOs, if the magnetic QW is (a) $i = 1$, (b) $i = 25$

Phase Diagram

For $N_D = 10^{10}\text{cm}^{-2}$, SSCOs appear in several intervals of the average field (6), $\phi_{\alpha,k}^N < \phi < \phi_{\omega,k}^N$, $k \in [1, 2, \dots]$. The number and width of these intervals of oscillatory solutions depend on N , as shown in Fig. 3, where $\phi_{\alpha,k}^N$ and $\phi_{\omega,k}^N$ are marked with triangles and inverted triangles, respectively. We observe that the sequence of ϕ at which oscillations appear can be approximated by the formula $\phi_{\alpha,k}^N = 38k/(N + 1)$, which provides the solid lines in Fig. 3.

Current-Voltage Characteristics

As can be seen in Fig. 3, the first bias interval for which there are SSCOs is the widest. For instance, for $N = 8$ this interval is $2.59 < \phi < 5.04$. The current-voltage characteristics (I-V) for a 8-period MQWS is depicted in Fig. 4, in which we show the maximum and minimum values of the current during SSCOs for biases in the voltage intervals $(\phi_{\alpha,k}^8, \phi_{\omega,k}^8)$, $k = 1, \dots, 5$.

Stationary States

As a general rule, the stationary states for $\phi < \phi_{\alpha,1}^N$ and for $\phi_{\omega,k_{max}}^N < \phi$ are spatially almost uniform. In the other stationary intervals of the I-V diagram, the profiles of F_i , P_i and n_i^\pm are not uniform and there are two EFDs, a low field domain adjacent to the cathode and a high field domain that extends to the anode, separated by a domain wall in which the field increases.

SSCOs

Examples of SSCOs for long MQWS are shown in Fig. 5 when only one well is magnetic. We have found that if the only magnetic QW is the i th (with $1 \leq i < N - 3$), the charge dipoles are emitted at this well, and dipole motion is limited to the last $N - i$ QWs.

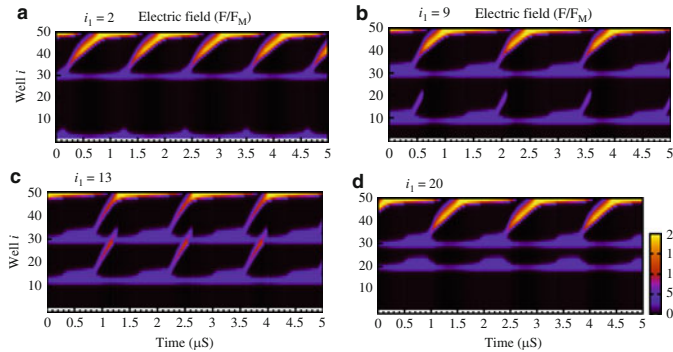


Fig. 6. Density plot of the electric field profile during SSCOs for $N = 50$ and DMS MQWS at $i_2 = 30$ and: (a) $i_1 = 2$, (b) $i_1 = 9$, (c) $i_1 = 13$, (d) $i_1 = 20$

MQWS with Two Magnetic Quantum Wells

MQWS with two QWs containing magnetic impurities exhibit a very rich dynamical behavior. Figure 6 shows the density plot of the electric field profile during SSCOs for a 50-well structure having two magnetic QWs. We have: (a) and (d) inhibition of dipole triggering at the first magnetic QW; (b) short and (c) long movements of the dipole waves.

4 Conclusions and Further Work

We have studied the dynamical behavior of MQWS with DMS in at least one QW. Spin oscillators may be designed using the results for short devices while long devices exhibit interesting patterns. Future work will explore switching the magnetic field through Δ .

References

1. Bandyopadhyay, S., Cahay, M.: Introduction to Spintronics, 2nd edn. CRC, Boca Raton (2008)
2. Zutic, I., Fabian, J., Das Sarma, S.: Rev. Mod. Phys. **76**, 323 (2004)
3. Sánchez, D., MacDonald, A.H., Platero, G.: Phys. Rev. B **65**, 035301 (2002)
4. Béjar, M., Sánchez, D., Platero, G., MacDonald, A.H.: Phys. Rev. B **67**, 045324 (2003)
5. Bonilla, L.L., Escobedo, R., Carretero, M., Platero, G.: Appl. Phys. Lett. **91**, 092102 (2007)
6. Bonilla, L.L.: J. Phys. Cond. Matter **14**, R341 (2002)